

Figure S1. Model orographic configuration for the late Miocene simulations. Writing indicates key palaeogeographic differences from the present day (discussed in the main text).

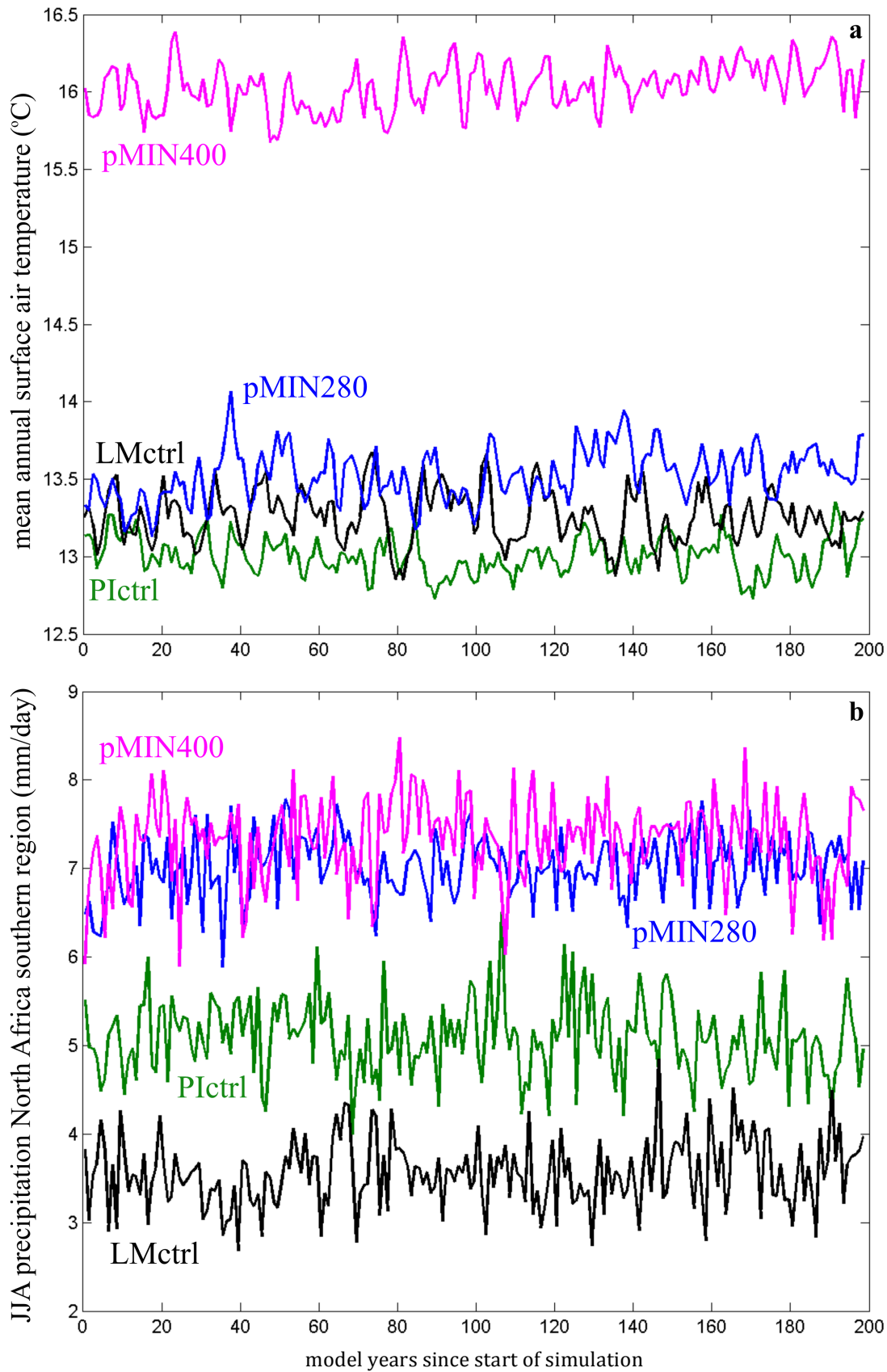


Figure S2. (a) Global surface air temperature trends and (b) JJA precipitation trends in the Southern region of North Africa through the 200 years of simulation for the preindustrial control (green line), late Miocene control (black), precession minimum at 280 ppm CO₂ concentration (blue) and precession minimum at 400 ppm CO₂ (magenta).

Calendar effect correction

As discussed in the main text, in the results presented in this study, the seasons are defined using a fixed present-day calendar. In order to evaluate the impact of using an angular calendar instead, we have applied a calendar effect correction to our results, using the method of Pollard and Reusch (2002). We note that we have used the same parabolic spline interpolation method as Pollard and Reusch (2002) but in our results a modification was applied to take into account a 360-day model year, where all months consist of 30 days.

Results after the calendar correction do not differ significantly for the variables discussed in this study and differences do not significantly affect the climate response. Some examples are shown in Figure S3 for precipitation in the North African monsoon region, which is of key interest in this work. We therefore present the uncorrected results in the main article, in order to facilitate comparison with other studies.

These differences will, however, not be negligible for seasonal comparisons with proxy data and potentially also for other variables not considered in this study. Figure S4 illustrates the more significant effect of the calendar correction on insolation at the top of the atmosphere.

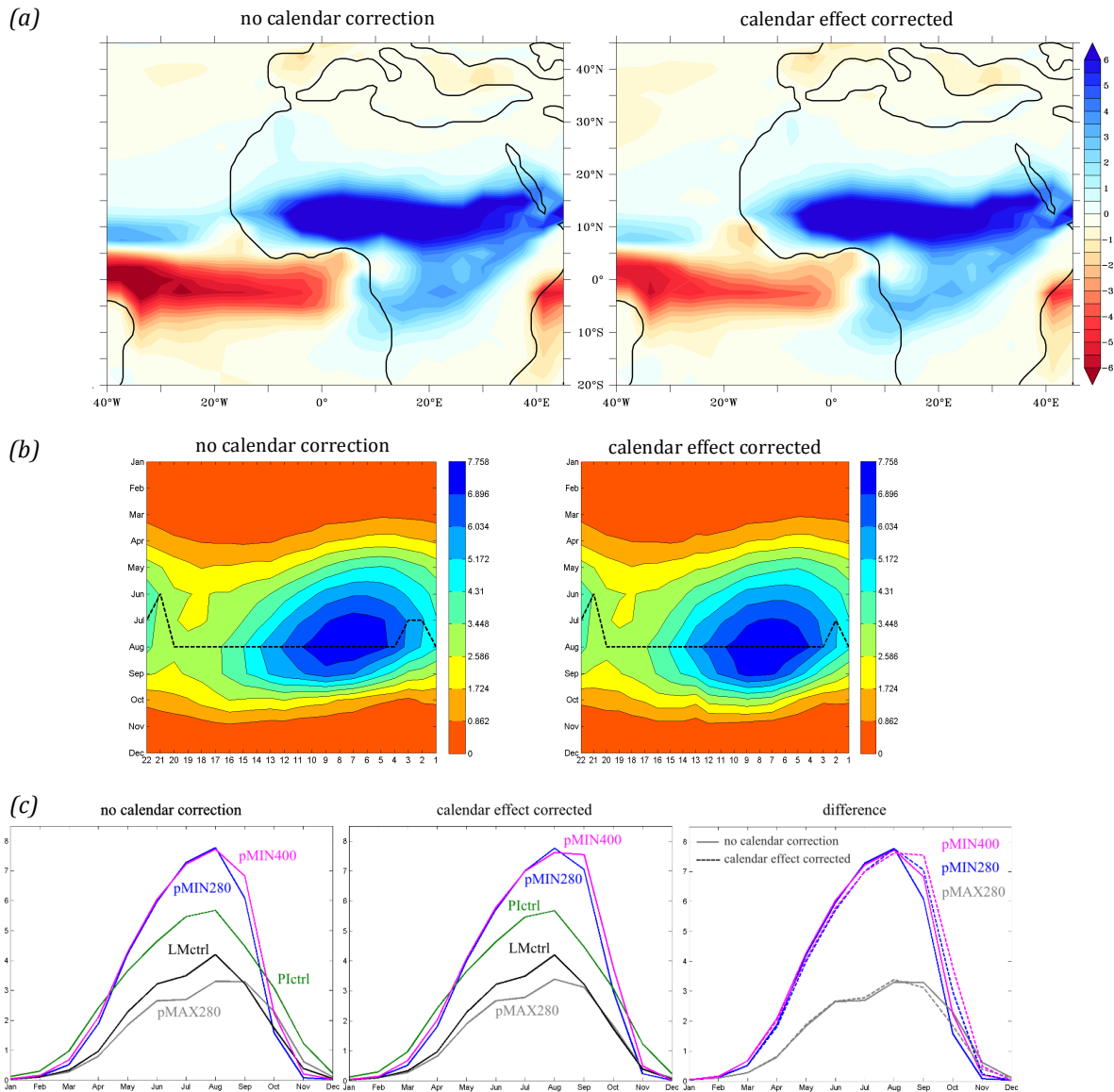


Figure S3. Calendar correction examples based on Figures (a) 9b, (b) 13d, and (c) 10d.

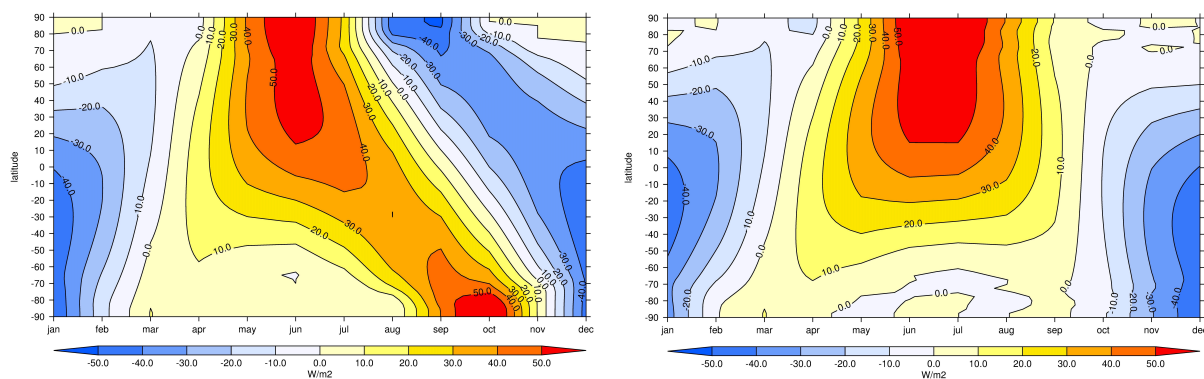


Figure S4. Top of the atmosphere incoming solar radiation (W m^{-2}) for experiment pMIN (shown as anomaly from present-day orbit), before (left) and after (right) calendar correction.

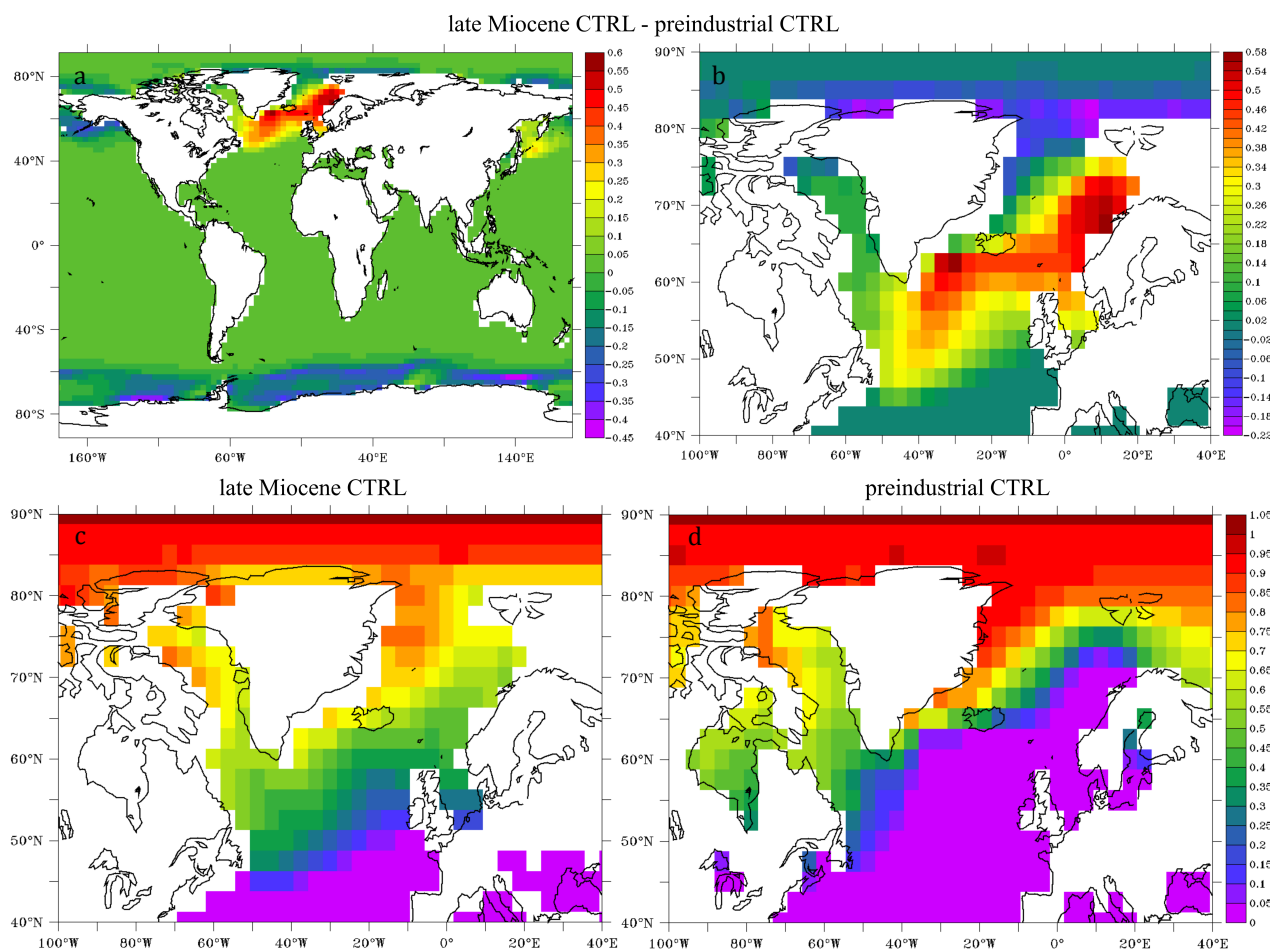


Figure S5. Differences in sea ice concentration (annual mean) between late Miocene and preindustrial control experiments for the a) globe and b) the North Atlantic. Absolute values of sea ice concentration in the North Atlantic are shown for both the (c) late Miocene and the (d) preindustrial simulations.

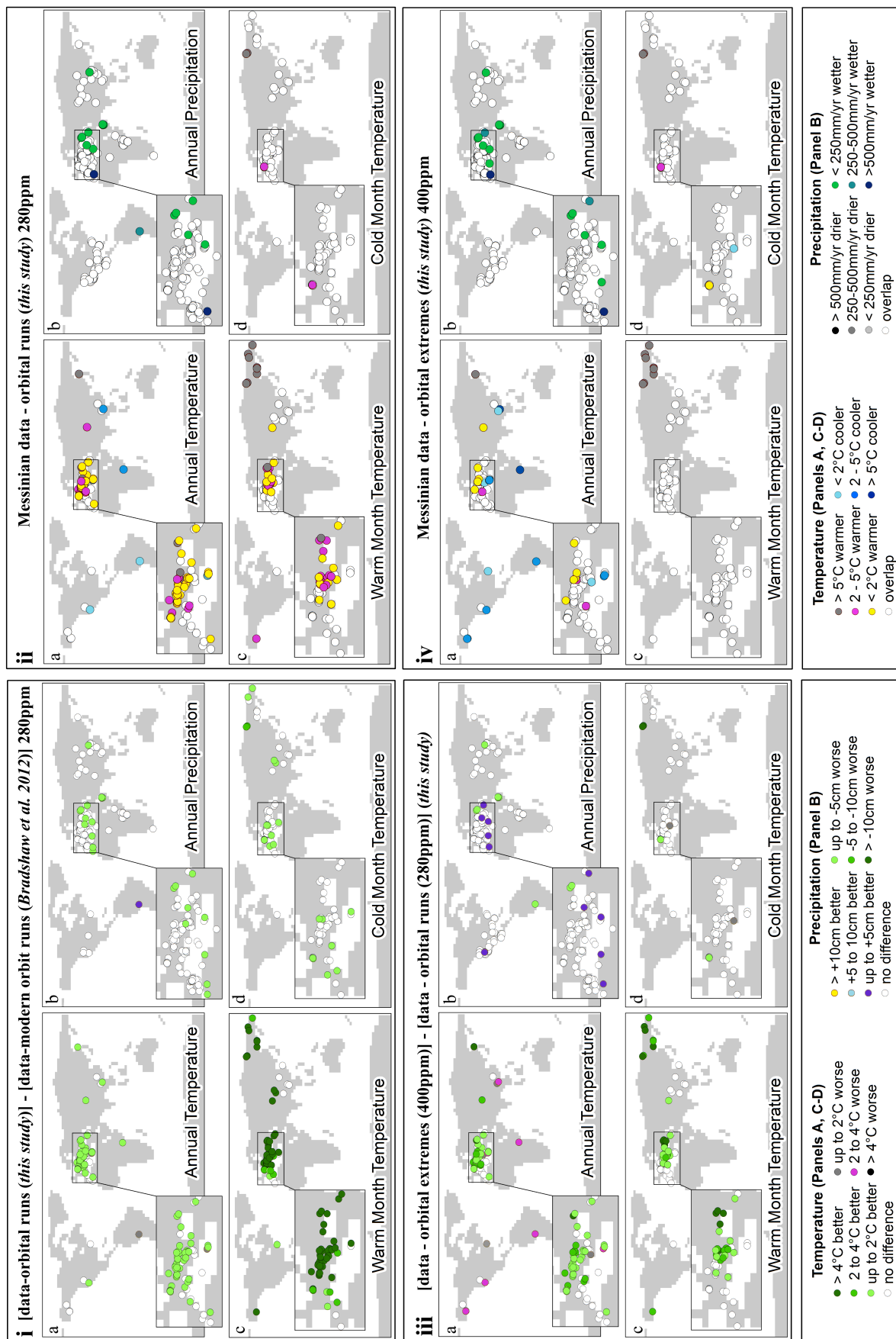


Figure S6. Figure 8 from the main article modified for colour-blind readers.

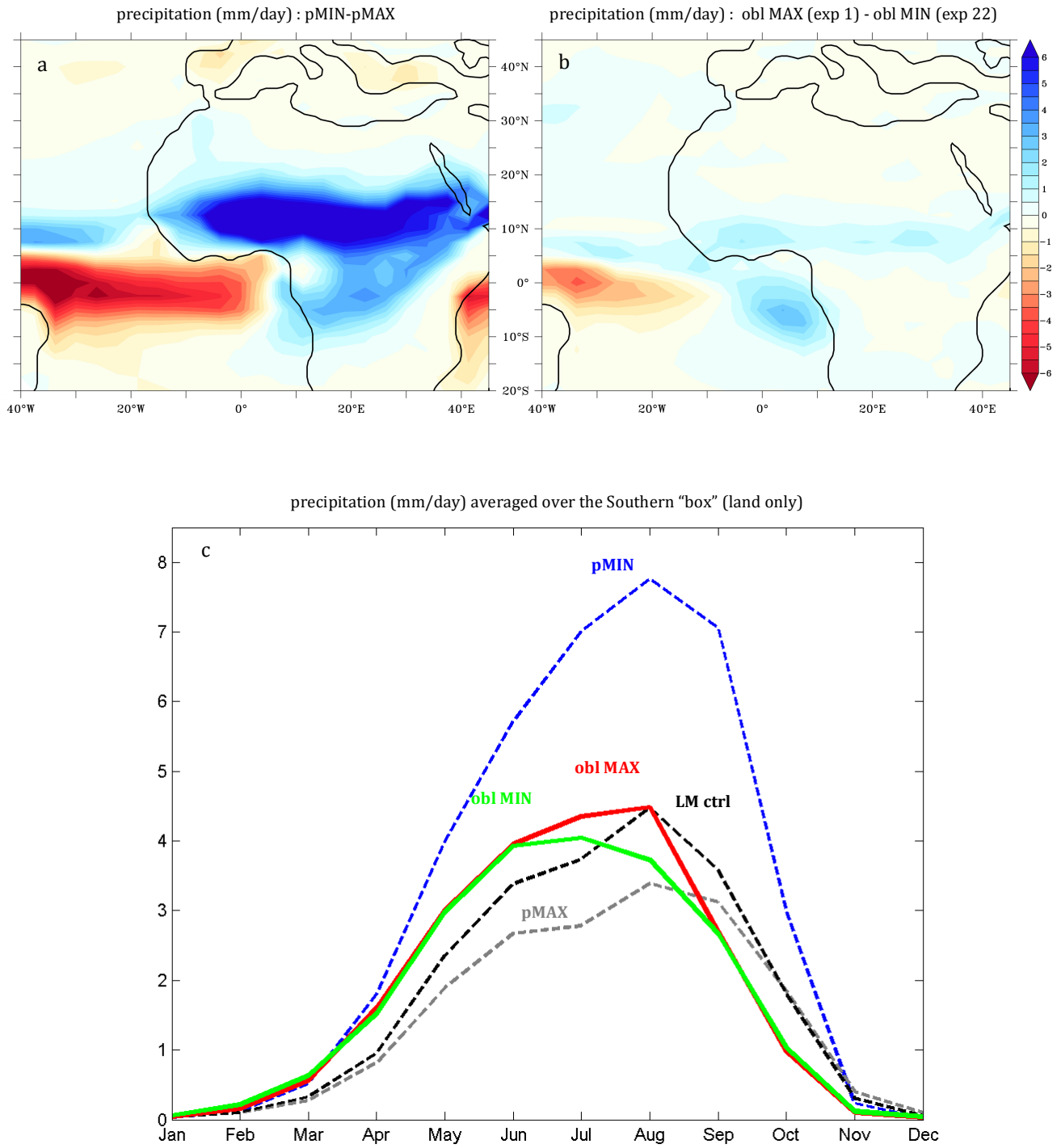


Figure S7. Seasonal precipitation distribution averaged over the southern "box" (land only) for obliquity minimum (green line) and obliquity maximum (red), compared with precession minimum (blue), precession maximum (grey) and late Miocene control (black) experiments. This is a modified version of Figure 10d from the main article.

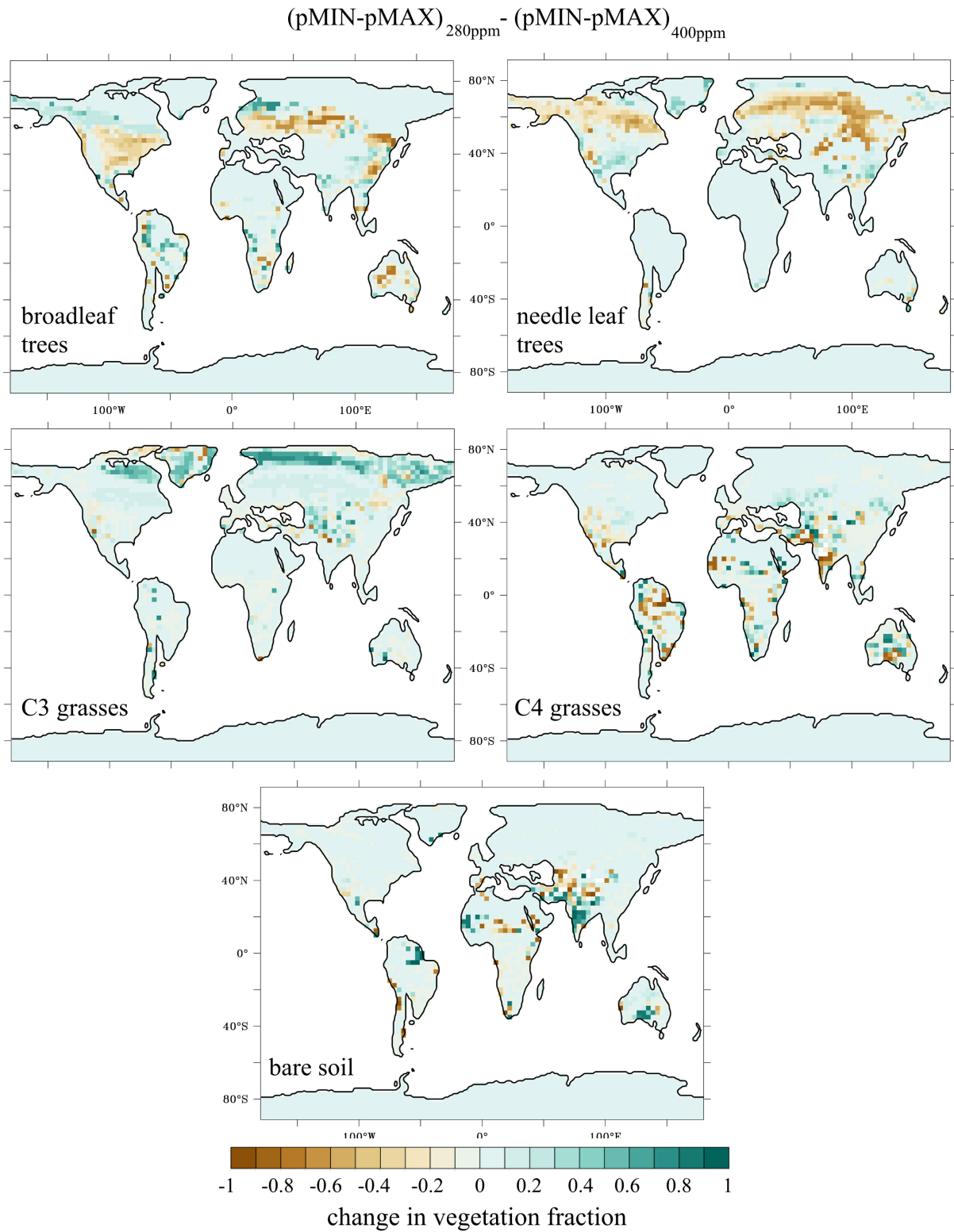


Figure S8. Vegetation fraction difference between precession minimum and precession maximum at 400 ppm CO₂ concentration minus the same difference at 280 ppm CO₂ for five different functional types. This is the global version of Figure 12 from the main article.

pMIN - pMAX 280ppm

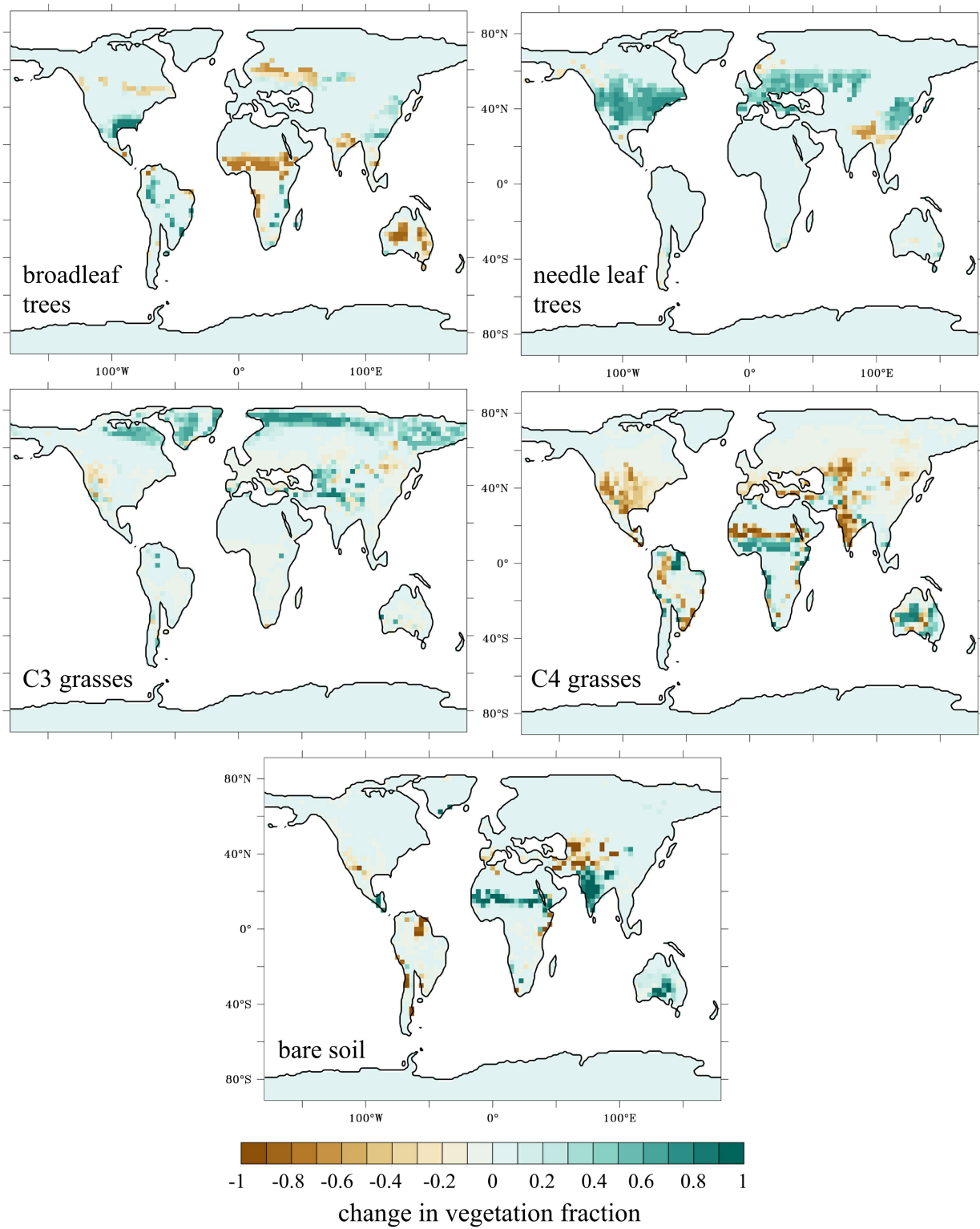


Figure S9. Global differences in vegetation fraction between precession minimum and precession maximum with 280 ppm CO₂ concentrations.

pMIN - pMAX 400ppm

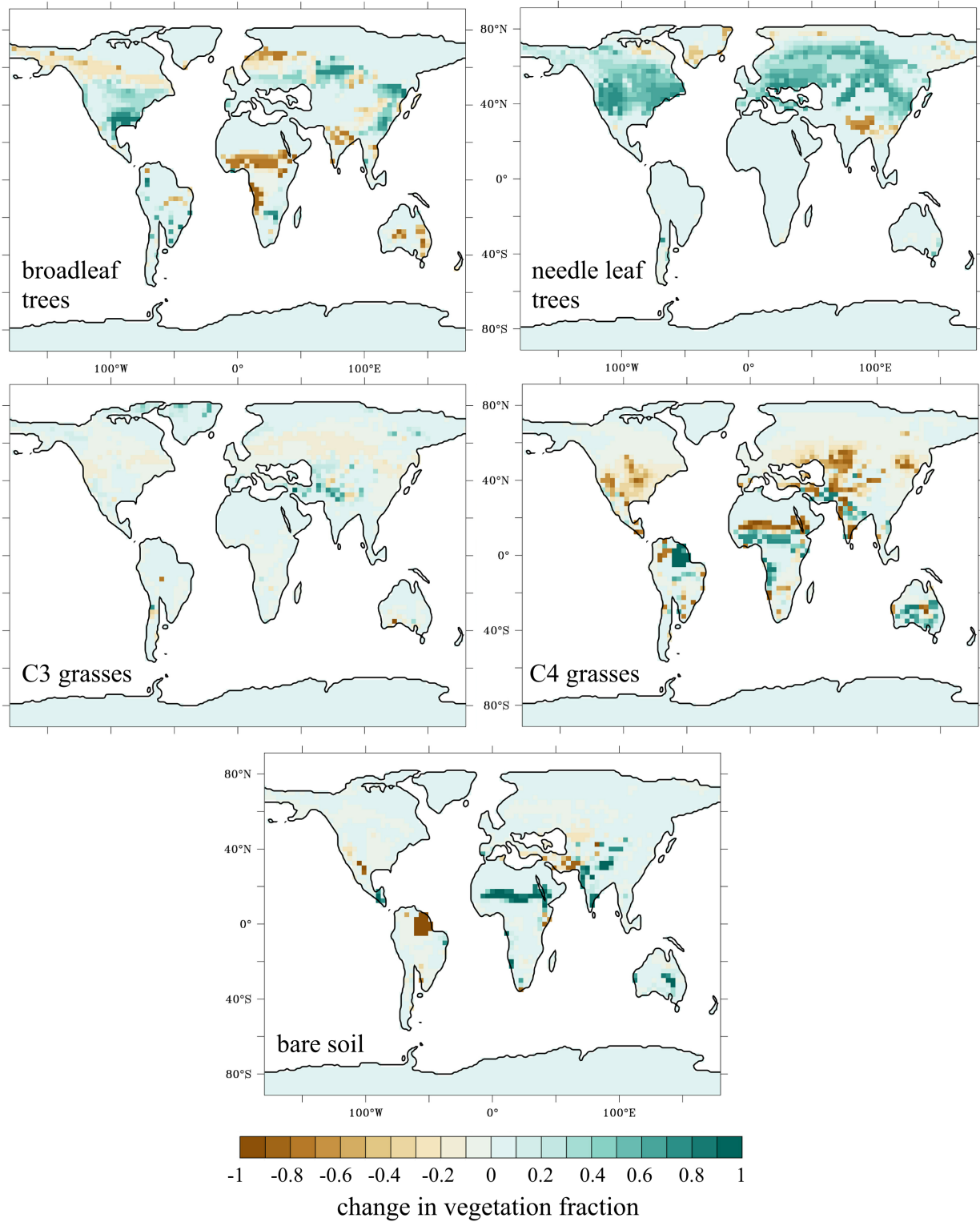


Figure S10. Global differences in vegetation fraction between precession minimum and precession maximum with 400 ppm CO₂ concentrations.

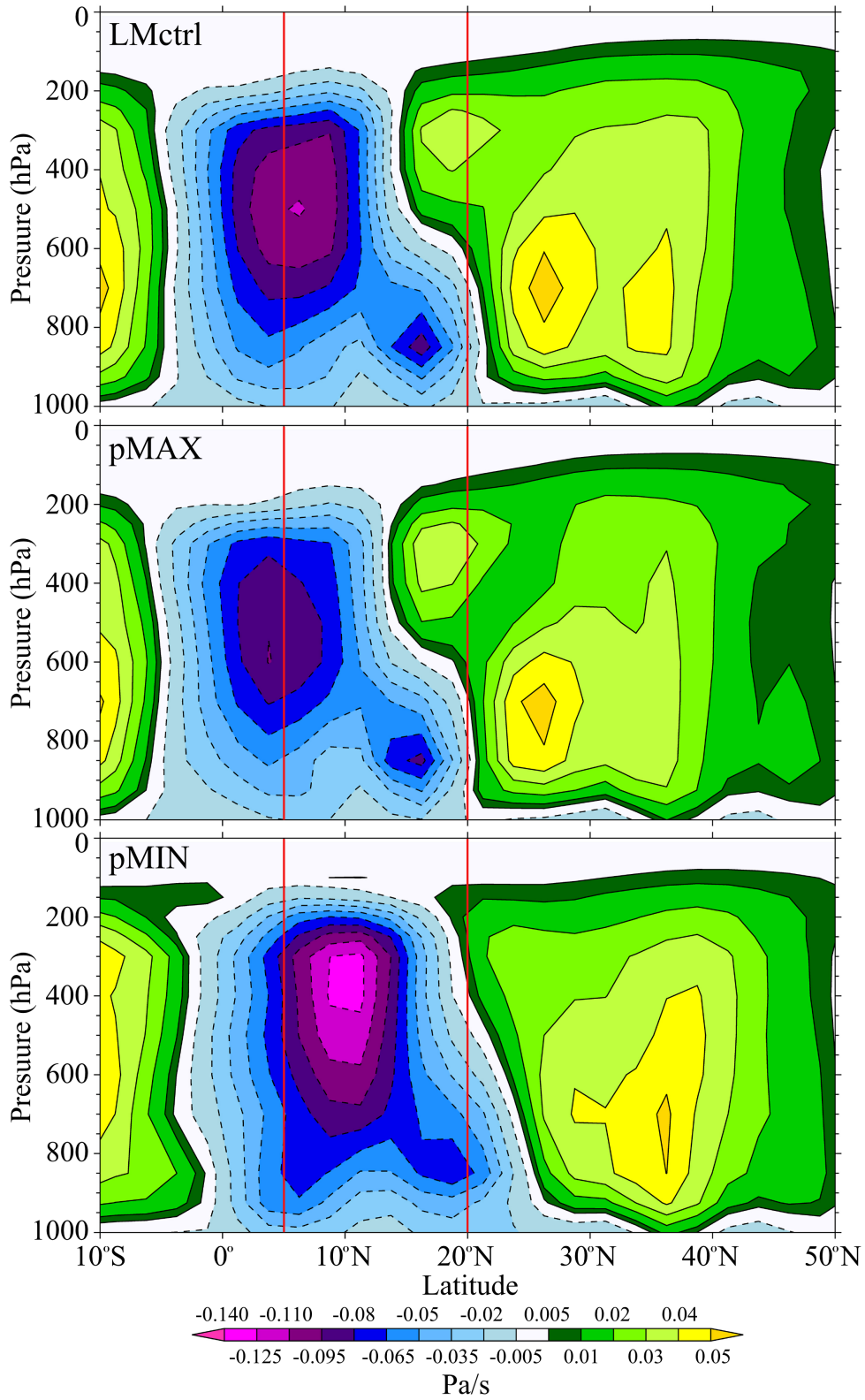


Figure S11. Hadley Circulation. Vertical velocity (ω) in Pa/s averaged longitudinally within the Southern "box" (as defined in Figure 9a). Negative values indicate vertical ascent and positive values indicate vertical descent. Note that the scale varies between positive values, where the increment is 0.01 Pa/s, and negative values, where the increment is 0.015 Pa/s. The red vertical lines indicate the location of the North Africa Southern "box", between 5 and 20°N.